Recovery boiler back-end heat recovery

JUSSI SAARI, JUHA KAIKKO, EKATERINA SERMYAGINA, MARCELO HAMAGUCHI, MARCELO CARDOSO, ESA VAKKILAINEN, AND MARKUS HAIDER

ABSTRACT: Sustainability and efficient use of resources are becoming increasingly important aspects in the operation of all industries. Recently, some biomass-fired boilers have been equipped with increasingly complex condensing back-end heat recovery solutions, sometimes also using heat pumps to upgrade the low-grade heat. In kraft recovery boilers, however, scrubbers are still mainly for gas cleaning, with only simple heat recovery solutions.

In this paper, we use process simulation software to study the potential to improve the power generation and energy efficiency by applying condensing back-end heat recovery on a recovery boiler. Different configurations are considered, including heat pumps. Potential streams to serve as heat sinks are considered and evaluated. Lowering the recovery boiler flue gas temperature to approximately 65°C significantly decreases the flue gas losses. The heat can be recovered as hot water, which is used to partially replace low-pressure (LP) steam, making more steam available for the condensing steam turbine portion for increased power generation. The results indicate that in a simple condensing plant, some 1%–4% additional electricity could be generated. In a Nordic mill that provides district heating, even more additional electricity generation, up to 6%, could be achieved. Provided the availability of sufficient low-temperature heat sinks to use the recovered heat, as well as sufficient condensing turbine swallowing capacity to utilize the LP steam, the use of scrubbing and possibly upgrading the heat using heat pumps appears potentially useful.

Application: Process models were developed and several cases were simulated to gain insight into potential power generation improvement through condensing back-end heat recovery, as well as the necessary preconditions for the potential to be realized.

A considerable amount of energy in conventional boilers is lost with the flue gases released through the stack to atmosphere. In the past, to avoid dewpoint corrosion, mills have maintained exit temperatures well above 110°C [1]. By cooling the flue gases further, some of this can be recovered [2]. Additional savings can be achieved if exiting flue gases are cooled below the dewpoint. The mass flow rate of the flue gas is reduced, and the latent heat of condensation can be recovered. Due to the combination of low temperature of the energy recovered and the cost of the materials required to prevent corrosion problems, this was not common in the past.

In recent years, the increased emphasis on energy efficiency and renewable energy has created interest in low-grade heat recovery by flue gas condensation in a variety of applications. Han et al. studied water and heat recovery in a large-scale power plant application utilizing high-moisture lignite fuel [3], obtaining 1.1%–1.5% electrical efficiency gains in different combinations of lignite dryer and flue gas condensing heat recovery systems. Liu et al. investigated a packed bed scrubber for coal-fired power plants with an oxy-fuel carbon capture and storage (CCS) system and a normal air-combustion boiler to determine optimal liquid-to-gas ratios [4]. Hebenstreit et al. performed a techno-economic study of small-scale biomass boilers with heat recovery by flue gas condensation including a heat pump; while comparatively short payback periods were obtained for chip-fired 10 MW boilers, profitability was poor-to-nonexistent for small-scale 10–100 kW pellet boilers [5]. Terhan and Comakli performed design and economic analysis of a tubular flue gas condensers in a 60 MW gas-fired boiler [6], obtaining a very short payback period of only one year. In Scandinavia, increasing numbers of biomass-fired boilers are being equipped with condensing back-end heat recovery systems, similar to that presented by Teppler et al. [7]. A shared characteristic of the aforementioned applications is high flue gas moisture, whether due to fuel moisture (biomass or lignite), hydrogen in the fuel (natural gas or biomass), or lack of atmospheric nitrogen (oxy-combustion).

The condensation itself can be either by surface heat exchanger, such as those considered in [6], for example, or in a direct-contact quench scrubber where cold water is sprayed on the flue gas. Depending on the temperatures and water content in the flue gas, vapor in the gas can condense on the droplets, or the droplets can evaporate into the flue gas. A cocurrent scrubber with evaporation can precede a countercurrent heat recovery quench scrubber [8]. Direct-contact quench scrubbers are often equipped with packed-bed columns where the spray flows over plastic or ceramic bed elements to maximize the contact area with water [4]. Three examples of condensing heat recovery implementation are presented in **Fig. 1**.

Different heat sinks have been considered for the recov-

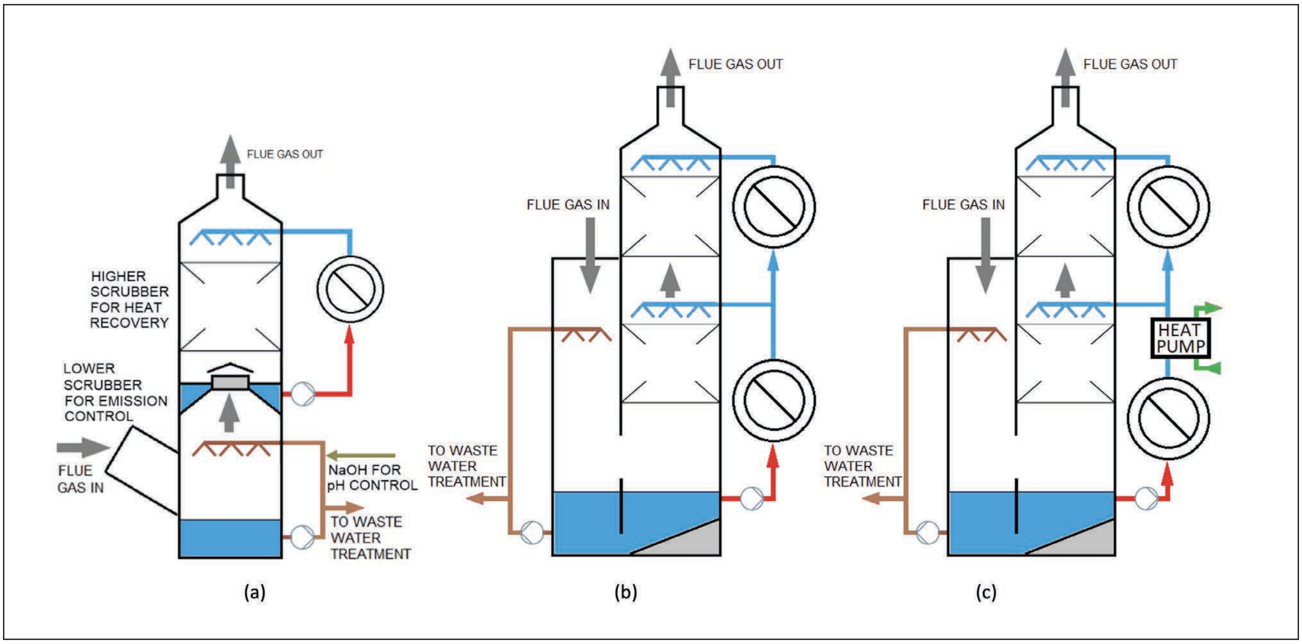

1. Three possible low-temperature heat recovery scrubber configurations: (a) 1-stage heat recovery scrubber, S1; (b) 2-stage heat recovery, S2; and (c) 2-stage with heat pump S2+HP.

ered heat; some studies have focused on boilers for district heating (DH), where the return water from the DH network is the heat sink, while in [3] the main condensate stream of a power plant steam cycle was identified as a potential heat sink. While the water vapor in flue gases typically has a considerable amount of latent heat available, the dewpoint sets an upper limit to the temperature of the recovered heat. This restricts the possible heat sinks in all applications. To circumvent this limitation, many studies, including [3,5,7], have considered heat pumps as a way to increase the possibilities for heat recovery. Both compression and absorption heat pumps have been installed in several operational boilers for DH generation in Scandinavia.

The purpose of this study is to investigate the theoretical technical potential of kraft recovery boiler waste heat recovery through flue gas condensation. The study is limited to direct-contact condensation in countercurrent packed bed quench scrubbers. Configurations presented in Fig. 1 are considered, using different heat sinks for the recovered heat, both as a retrofit to an existing mill and in a newly built mill context.

METHODS

In this study, we consider the case of a large Nordic pulp mill, broadly similar to that described by [9]. The annual pulp production is 1.6 million air-dried (a.d.) metric tons during an operating time of 350 days per year, consuming 0.83 MWh/a.d. metric ton of 12 bar(a) medium-pressure (MP) steam and 1.8 MWh/a.d. metric tons of 5 bar(a) low-pressure (LP) steam. Black liquor production is 1.5 metric tons black liquor/a.d. metric ton; the black liquor composition is listed in **Table I**.

We have modeled the boiler, steam cycle, and the heat recovery equipment using IPSEpro, a steady-state equation-based simulation software from SimTech (Graz, Austria). IPSEpro comes with a module development kit (MDK) for creating new component modules not included in the standard library. Several different sub-cases are evaluated, differing in steam cycle configuration and in heat recovery. These are summarized in **Table II** and described in more detail in the following sections. Only design point operation is considered; the effects of possible variations of liquor and/or air flow are ruled beyond the scope of the study.

Flue gas cooling

As the flue gases are cooled down further after the economizer, only the sensible heat of the gas stream is transferred at first. This continues until water dewpoint is reached, typically at approximately 70°C, as seen in **Fig. 2**. During this first noncondensing heat recovery stage,

Na	K	Cl	C	H	N	O	S
0.2074	0.0259	0.0033	0.3152	0.0319	0.0009	0.3605	0.0542

Na = sodium; K = potassium; Cl = chlorine; C = carbon; H = hydrogen; N = nitrogen; O = oxygen; S = sulfur.

I. Black liquor composition (kg/kgds).

Steam Cycle Case	C	DH
LP turbine(s)	Conventional condensing	Parallel condensing and district heat (DH) turbines on the same shaft
DH generation	None	90 MW, 2-stage extraction + back pressure steam from the DH turbine

Heat Recovery Case	D	S1	S2	S2+HP
Description	**Base case**	**1-stage scrubber**	**2-stage scrubber**	**2-stage scrubber with heat pump**
Hot-water non-condensing heat exchanger	yes	yes	yes	yes
Venturi scrubber	-	yes	yes	yes
Packed-bed scrubber	-	yes	yes (two)	yes (two)
Combustion air humidifier	-	-	yes	yes
Heat pump	-	-	-	yes

II. Summary of considered cases; all 4 heat recovery cases are simulated with both steam cycle cases.

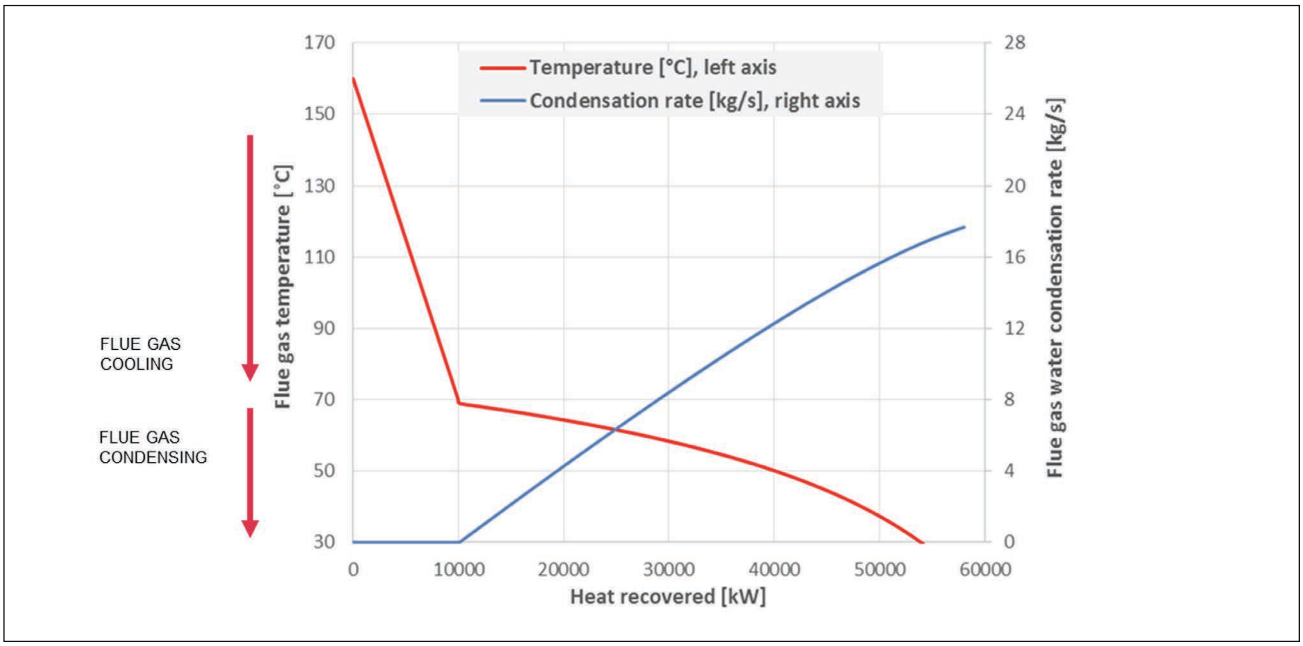

2. Cooling recovery boiler flue gases in a sample case.

the flue gases are typically cooled in an indirect arrangement using water as the heat transfer medium; flue gases transfer heat to the water inside a heat transfer surface, and the heated water is then used to heat the target media (e.g., combustion air or DH water) in another heat exchanger [2].

The last part of heat recovery involves water condensation in addition to continued cooling; the condensation allows much more heat to be recovered. Often, the condensation is implemented in a scrubber. The flue gases still contain impurities and thus cannot be allowed in direct contact with the heat sink fluids. An indirect connection is thus implemented by using the heated scrubber water collected at the bottom as an intermediate medium, and this water is pumped through heat exchangers transferring heat to the intended heat sink streams.

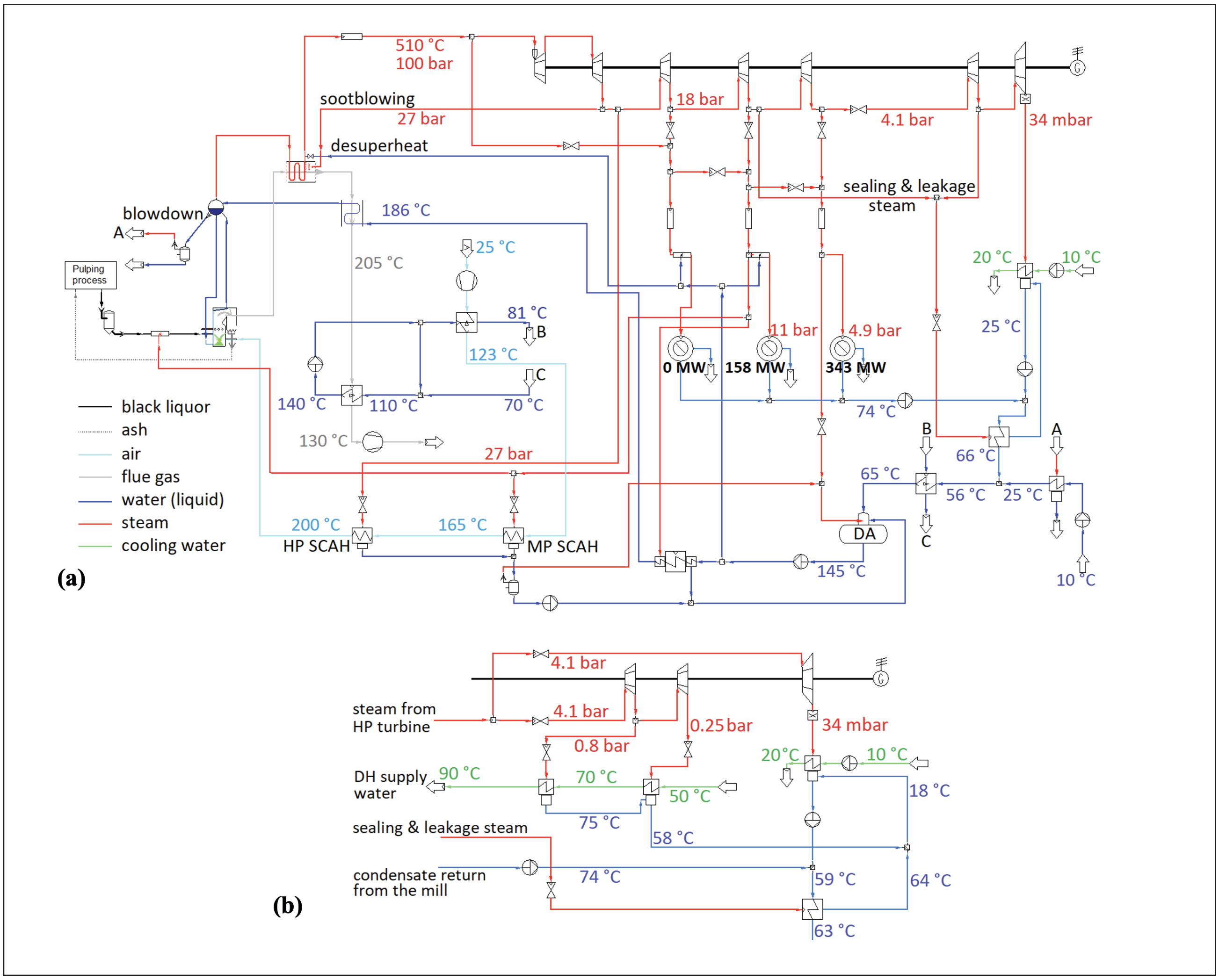

3. Flowsheet models of (a) the baseline Case C-D, with condensing turbine, dry heat recovery; and (b) turbine back-end of Case DH-D, with two-part turbine low pressure end with parallel district heating (DH) and condensing turbines. (HP = high pressure; MP = medium pressure; SCAH = steam coil air heater.)

Cases studied

Two variants of the plant are considered: Case C (**Fig. 3a**) uses all steam remaining after the LP steam demand for producing electricity at the condensing turbine. Case DH is co-located at a large North European municipality and produces 90 MW of DH; the turbine low pressure part is depicted in Figure 3b, otherwise case DH is identical to Case C.

All cases have a modern boiler with main steam parameters of 100 bar(a) and 510°C. A high-pressure feedwater preheater is used to heat the boiler feedwater to 186°C before the economizer. Flue gas temperature after the economizer is approximately 205°C.

Four different heat recovery schemes are considered after this: the dry scheme ("D") is the basic case where the flue gas stream is cooled to 130°C–140°C using a 110°C inlet temperature water loop. The water is heated to 140°C, and the hot water is used for heating combustion air and the main condensate stream. The 70°C return water is then heated to 110°C inlet temperature by mixing it with a fraction of the 140°C outgoing water. Maintaining sufficiently high inlet temperature prevents condensation at the surfaces.

The scrubber scheme ("S1" in Fig. 1) has a simple heat recovery scrubber, where a packed-bed spray tower is used to condense the flue gas moisture for heat recovery. The scrubber scheme S1 is limited by the availability of low-temperature heat sinks. To overcome this limit, utilizing condensed water to moisturize incoming air is considered as an additional heat sink, implemented in a two-stage scrubber ("S2"), where water from the second, colder scrubber is used for the combustion air humidifier (CAH). Finally, a heat pump (HP) can be added to upgrade the recovered heat to a higher temperature, increasing the availability of possible heat sinks. This is considered in conjunction with the humidification in case "S2+HP".

Boiler model

The recovery boiler model is based on a furnace module, followed in flue gas flow direction by separate heat exchanger modules representing the superheater, economizer, and a hot-water heat recovery heat exchanger after the electrostatic precipitators. Air preheating takes place with steam. The heat losses with ash, smelt, reduction reactions, and radiation losses are determined in the furnace model that was developed using the IPSEpro MDK kit.

The calculation methodology is based on [10], assuming a firing liquor dry solids content of 0.83 and temperature of 140°C. The furnace module calculates the higher heating value (*HHV*) of the black liquor according to [11]:

$$HHV = 25.040\ C_C + 0.1769\ C_S - 2.582\ C_{Na} + 48.920\ C_H + 4.231 \tag{1}$$

where C_x is the mass fraction of species x in the dry solids (kg_x/kg_{ds}). Black liquor enthalpy h_{bl} (kJ/kg) is determined as in [12], and first, the enthalpy at 80°C is obtained according to [13]:

$$h_{bl}(80°C) = h_{H_2O}(80°C) + 105\,\frac{kJ}{kg}\cdot\left(e^{\frac{x_{ds}}{0.3}} - 1\right) \tag{2}$$

where x_{ds} is the black liquor dry solids fraction, and this is corrected to actual temperature with a correlation for $c_{p,bl}$ (kJ/kgK) by Masse et al. [14] as cited in [11]:

$$\begin{aligned} c_{p,bl} &= 4.216\cdot(1 - x_{ds}) + (1.675 + 0.00331\,t)\cdot x_{ds} \\ &\quad + (4.87 - 0.02\,t)\cdot(1 - x_{ds})^{x_{ds}^3} \end{aligned} \tag{3}$$

where t is temperature (°C).

The calculation of the flue gas, ash and smelt compositions is based on balances according to [10], using reduction efficiency of 0.94 and an excess air ratio of $\lambda = 1.18$, resulting in oxygen and moisture contents of 2.5% and 13.4% by mass, respectively, before the sootblowers. The values of reduction efficiency and excess air ratio have considerable impact on the thermal power of the boiler and thus the power generation in the plant. Their effect on the performance gain obtained through the use of the condensing back-end heat recovery is only very little, however. The small effects come through the changes in the condensate stream from the condensing turbine, an increase of which allows slightly greater heat recovery and thus slightly greater benefit from the condensing scrubber, as well as slight variations of flue gas moisture and thereby dewpoint temperature.

For smelt and ash, specific heats of 1.42 and 1.2 kJ/kgK are assumed, respectively. Ash composition is determined according to [10], and the main components are listed in **Table III**. The ash is mixed with the black liquor (Table I) in the evaporator plant.

The flue gas stream exits the furnace module at a temperature of approximately 1100°C. It should be noted that the furnace model is a mass and energy balance model of combustion, reduction, and steam generator heat transfer, and does not consider, e.g., temperature profiles or radiation heat transfer into the superheaters. The boiler bank is also omitted in the model. The simplified furnace/superheater modeling and the placement of all steam generator surfaces in the furnace in the absence of a boiler bank are sufficient for the purposes of this study, as they do not affect the overall mass and energy balances of the boiler, steam generation, or the back-end heat recovery. Temperature difference at the superheaters is affected and thus superheater area, but for the purposes of this study, this has no effect.

The economizer and superheater models are otherwise similar to those described in [15] for a fluidized bed boiler, but they include the soot blowing steam becoming mixed with the flue gas flow. The sootblowers use 2.7 MPa(a) extraction steam from the turbine. Steam coil air heaters (SCAHs) pre-heat the 25°C ambient air to 200°C before the boiler. Air heating is performed in multiple stages, with a SCAH using 2.7 MPa(a) steam as the final stage. Earlier stages are implemented using 1.1 MPa(a) MP steam and hot water that has been heated with flue gas. Heat from the scrubber is used in addition to these stages, either in an additional heat exchanger preceding the aforementioned

Element	Per Liquor, $kg/kg_{BL,ds}$	Composition, kg/kg	Flow with Ash, kg/s
Na	0.0317	0.320	2.795
K	0.0059	0.059	0.518
Cl	0.0012	0.012	0.108
S	0.0133	0.134	1.17
C	0.0035	0.035	0.309
O	0.0434	0.438	3.823

Na = sodium; K = potassium; Cl = chlorine; C = carbon; H = hydrogen; N = nitrogen; O = oxygen; S = sulfur.

III. Ash composition.

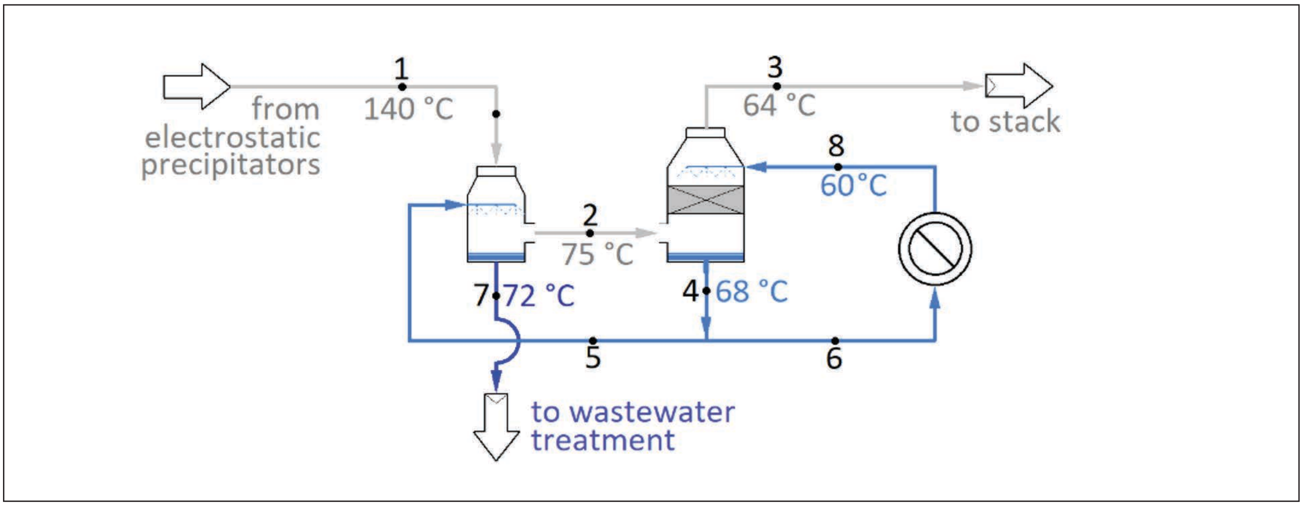

4. Heat recovery scheme with flue gas (1) entering a venturi scrubber (VS). Cooled flue gas at increased moisture (2) enters the packed bed scrubber (HRS), and exits to the stack (3). Liquid water from VS (7) is sent to wastewater treatment; liquid from HRS (4) is used for VS spray (5) and for heat consumers (6).

ones, or in a humidifier where scrubber water is sprayed into the air stream.

The steam cycle models are based on those presented in [15]. The work stages of the turbine have isentropic expansion efficiencies of a $\eta_s = 0.88$ (dry) at optimal flow rate. The work stage modules calculate the efficiency variation due to mass flow rate change according to a correlation from Jüdes et al. [16]. The effect of moisture at the end of expansion is estimated according to [17]. The variation of pressure ratios as a function of mass flow rate is modeled with the ellipse law by Traupel [18]. Expansion ends at a condenser with 3300 m^2 area and 2.9 kW/m^2K overall heat transfer coefficient at design conditions of 25 mbar, 50 kg/s steam, and 2500 kg/s coolant flow. Detailed descriptions of the turbine models and condenser off-design model can be found in [15].

A turbine sealing steam flow of 0.5% of the average flow through the high-pressure turbine is assumed to be fully recovered and used for condensate pre-heating, together with the hot-water boiler back-end heat recovery scheme heating the main condensate to 65°C before the 4.2 bar(a) deaerator. The final stage of feedwater heating is the 1310 m^2 HP high-pressure feed heater operated with 11 bar steam for a terminal temperature difference (TTD) = 1°C and a 186°C, 116 bar(a) final feedwater state before the boiler.

Heat recovery component models

A condensing heat recovery can be implemented in many ways: surface condensers or scrubbers can be used, there can be multiple stages, and heat pumps can be used to increase the temperature level of recovered heat and thereby the selection of possible sinks to which the heat can be recovered. Within the scope of this work, we considered scrubbers. A typical configuration of such includes two different components, each with their own functions:

- Packed-bed heat recovery scrubber, referred to as HRS
- Venturi scrubber, referred to as VS

A simple configuration depicting both components as implemented in the configuration S1 is seen in **Fig. 4**. The HRS is the main heat recovery component, where cold water is sprayed from above counterflow to the upwards-flowing flue gas. A packed bed of filler elements provides an increased contact area for water and gas. Moisture in the flue gas condenses on the spray droplets, as well as on the water pellicle formed on the packed bed filler elements. The flue gas typically exits the tower at a temperature slightly higher than the spray water temperature. The temperatures in Fig. 4 indicate typical values possible for such equipment and not precisely any one particular result of the cases studied here.

A separate co-flow VS can be used before the HRS, as depicted in Fig. 4. The role of this scrubber differs from the HRS. The temperature of the flue gas entering the VS is usually far higher than the dewpoint and also too high to permit low-cost lightweight materials for the packed bed to be used in the HRS. By spraying water taken from the bottom of the HRS device into the flue gas, evaporation, rather than condensation, will take place, which cools the flue gas, increases the moisture content, reduces the volumetric flow rate, and cleans the gas. This permits a smaller HRS stage using cheaper materials and less fouling in the heat exchangers. Although there is net energy transferred into the flue gas through evaporation rather than being recovered from it, this will not reduce overall efficiency, as the latent heat of evaporation will be recovered through condensation in the HRS. In addition to cooling and moistening, the VS also serves as the final gas cleaning stage, and pH control by sodium hydroxide (NaOH) injection can also be implemented.

The mass flow rate of the spray is typically much less in the VS than it is in the HRS, and dewpoint temperature is unlikely to be reached; thus, only evaporation will take place. We estimated a flue gas exit temperature of $T_2 = T_{sat} + 5°C$, with a spray mass flow rate of $\dot{m}_5 = 0.5\dot{m}_1$. The overall performance results are not very sensitive to this temperature difference estimate, the magnitude of which is small compared to the temperature reduction from the 130°C–140°C VS inlet temperature to slightly over 70°C–80°C outlet temperature. The sensible heat of this temperature reduction is itself also less than the heat of evaporation, as some of the droplet liquid water is evaporated into the flue gas stream. The gross generator power changes only by 3–4 kW_{el} per 1°C change in the T_2 - T_{sat} temperature difference.

The water outlet temperature T_7 from the VS is typically very close to the wet bulb temperature T_{wb} [19]. The VS module calculates the T_{wb} by applying the analogy of heat and mass transfer, yielding a well-known equation:

$$T_{\mathrm{wb}} = T_{\mathrm{g}} - \frac{M_{\mathrm{H_2O}}}{\rho_{\mathrm{g}}\, c_{\mathrm{p,g}}} \cdot \frac{p_{\mathrm{g}}}{R_{\mathrm{u}} T_{\mathrm{g}}} \cdot Le^{1-n} \cdot h_{\mathrm{fg}}(T_{\mathrm{wb}}) \cdot \ln \frac{p_{\mathrm{g}} - p_{\mathrm{H_2O}}}{p_{\mathrm{g}} - p_{\mathrm{sat}}(T_{\mathrm{wb}})} \tag{4}$$

where R_u is the universal gas constant, T is the absolute temperature (K), h_{fg} is the water latent heat of evaporation, subscripts “g” and “H_2O” refer to mean wet flue gas conditions and water, respectively, and Le is the Lewis number:

$$Le = \frac{k_{\mathrm{g}}}{\rho_{\mathrm{g}} c_{\mathrm{p,g}} D_{\mathrm{AB}}} \tag{5}$$

where D_{AB} is the binary diffusion coefficient between water vapor and wet flue gas (m²/s), and k_g is the thermal conductivity of wet flue gas (W/mK). Flue gas properties are determined as mass-weighted sums of the properties of its components evaluated at film temperature. With the preceding assumptions and equations, and applying mass and energy balances, the model determines the flue gas exit temperature and the mass fraction of water in the gas.

Packed bed counterflow scrubber

The flow of spray water in the HRS is much greater than in the VS. While limited evaporation may take place at the bottom of the spray tower, the main mode of operation will be condensation of flue gas moisture on the spray droplets and on the water pellicle at the packing material surface. Flue gas relative moisture at the exit will be approximately 100%. The temperature difference of the exiting flue gas flow to the spray water, $\Delta T_g = T_3 – T_8$ in Fig. 4, can be affected by both spray water flow rate and the bed sizing. Optimal flow rate depends on the cost of packing material and desired flue gas outlet temperature; the higher the water/flue gas (W/G) ratio, the smaller the volume of packing material required for a given gas outlet temperature. Liu et al. [4] suggest W/G ratios in the order of 2.5 to 5 for conventional boilers; here, we used W/G = 5 and $\Delta T_g = 7°C$. Condensate exit temperature is estimated at 5°C below the saturation temperature corresponding to water vapor partial pressure, $T_4 = T_{sat}(p_{H2O,2}) – 5°C$.

Results and discussion

Models of the plant designs described previously were built in IPSEpro to evaluate their performances. The availability of large enough heat sinks in the system proved to be a limitation; for this reason, we used multiple heat sinks in designing the heat recovery configurations in the different cases: combustion air, the main condensate stream, and the makeup water.

Case C: conventional condensing turbine

Table IV lists the results from the simulations for Case C, the base mill where all excess LP steam is expanded through the condensing tail, with no additional external heat sales. In the base case C-D with dry heat recovery, there is 205 MW of net power generation ($P_{el,net}$) remaining after the boiler and steam cycle auxiliary consumption (P_{aux}) has been deducted that is available for use by the mill and for sales to the national grid.

The single-stage heat recovery scrubber (S1) increases the electricity production in a new mill by 3% (6.4 MW). In an existing mill that wants to retrofit the same, all the heat might not be recovered; with the parameters used in this study, we found heat overproduction and dumping of steam and a much smaller 1% (2.3 MW) net power generation gain.

If the combustion air is humidified, the CAH represents an additional sink for utilizing the low temperature heat recovered from the scrubber. In the simulation models, we diverted 40% of the scrubbing water, after being cooled in the heat exchangers, to the CAH. This spray water, further cooled by evaporation, is collected from the bottom of the CAH tower and sent to the final flue gas scrubbing spray stage. The humidification increases the heat capacity rate of the air and flue gas, and as a result, flue gas temperatures at the nose and before the boiler bank are reduced. The net outcome is very little gain in power generation for the retrofit scenario and a small net loss with the new mill one.

The poor performance of the combustion air humidification, at first seemingly contradictory to the common use of combustion air humidification in biomass boilers with flue gas condensation, is explained by the different combustion air preheating in recovery boilers. In a recovery boiler, air preheating is typically implemented with steam coil air heaters, including in the model we used in this study. As a result of humidification, the heat capacity rate of the combustion air increases. This increase is enough that, although air arrives at the SCAH at a higher temperature than it would without the CAH, more high- and medium-pressure extraction steam is needed to still reach the

	$T_{fg,out}$ °C	$q_{m,fg}$ kg/s	$q_{m,cond}$ kg/s	$q_{m,dump}$ kg/s	$q_{m,CT}$ kg/s	P_{aux} MW	P_{gen} MW	$P_{el,net}$ MW	ΔP_{el} MW
D	130.7	358.5	0	0	50.29	7.69	213.0	205.3	
S1 / retrofit	65.7	358.5	-1.6	5.58	55.73	8.58	216.2	207.6	2.3
S1 / new	66.1	358.5	0.1	0	59.25	8.13	219.9	211.8	6.4
S2 / retrofit	65.8	375.3	17.7	4.15	55.74	8.29	216.2	207.9	2.6
S2 / new	65.7	375.0	18.0	0	59.95	8.05	219.1	211.1	5.7
S2+HP* / retrofit	65.7	375.9	18.6	8.30	55.74	8.55	215.8	207.2	1.9
S2+HP** / new	64.0	374.0	22.4	0	65.90	10.87	223.7	212.8	7.4

* ΔT_{lift} = 20°C; coefficient of power (COP) = 9.0
** ΔT_{lift} = 30°C; COP = 6.3

IV. Pure condensing turbine, Case C. Heat recovery configurations S2 and S2+HP utilize the heat recovered from the second, colder scrubber stage for combustion air humidification.

	$T_{fg,out}$ °C	$q_{m,fg}$ kg/s	$q_{m,cond}$ kg/s	$q_{m,\ dump}$ kg/s	$q_{m,CT}$ kg/s	$q_{m,DH}$ kg/s	P_{aux} MW	P_{gen} MW	$P_{el,net}$ MW	ΔP_{el} MW
D	130.7	358.5	0	0	9.016	40.27	7.66	199.5	191.9	
S1 / retrofit	62.7	358.5	10.8	0	32.89	26.40	8.22	202.7	194.5	2.6
S1 / new	62.8	358.5	10.4	0	29.59	29.21	8.05	207.5	199.5	7.6
S2 / retrofit	60.6	386.7	44.7	0	36.78	22.68	8.39	207.3	198.9	7.1
S2 / new	60.6	386.6	44.6	0	35.31	24.01	8.42	209.9	201.4	9.6
S2+HP* / retrofit	58.5	383.5	46.1	0	42.34	23.29	11.41	211.4	200.0	8.1
S2+HP* / new	58.4	383.2	46.1	0	40.80	24.71	11.31	215.1	203.8	12.0

* ΔT_{lift} = 35°C; COP = 5.4

V. Parallel DH and condensing turbines, Case DH. Heat recovery configurations S2 and S2+HP utilize the heat recovered from the second, colder scrubber stage for combustion air humidification.

same final temperature. Better performance is achieved with the S1 scheme, where the air is preheated using hot scrubber water in a heat exchanger. The CAH operating parameters were 15°C temperature difference at the spray, a relatively small evaporation rate of 15–20 kg/s, and 98% humidity of air at the outlet. Increasing evaporation reduced the net power generation with both retrofit and new mill cases.

Finally, we tested the effect that could be had by using an ammonia (NH_3) compression heat pump to increase the temperature of the recovered heat in the 2-stage heat recovery scrubber case (S2+HP). Compression heat pump operating parameters are always a compromise between a high temperature lift ΔT_{lift} (permitting a high heat rate), and a high coefficient of power (COP): increasing one reduces the other. A rudimentary manual optimization was carried out to find the COP – ΔT_{lift} combination yielding the highest $P_{el,net}$ gain, and it can be seen that while a small gain could be achieved with the new mill case, the retrofit case resulted in yet more reduction over the S2. A reduction, as small as it was, was achieved with parameters corresponding to only 1 MW heat transfer. Increased heat transfer and ΔT_{lift} would only reduce $P_{el,net}$ further. This is unsurprising, as there would be no way to use the saved LP steam with the condensing turbine swallowing capacity already reached.

Case DH: district heat generation

The results from the simulations for the district heating mill where 90 MW of district heat is generated through a separate DH turbine are shown in **Table V**. In the base case DH-D, approximately 192 MW of electricity is produced when the mill is operating at design level. Adding the simple one-stage heat recovery scrubber (S1) can increase the electricity production in a new mill by 4% (7.6 MW). In an existing mill that wants to retrofit the same, the steam dumping can be avoided, in contrast to the pure condensing case C. On the other hand, the much-reduced steam flow through the DH turbine qm, DH reduces the pressure ratio in a turbine sized for a larger flow. This requires increased throttling and counters some of the power generation increase otherwise achieved through increased flow and reduced throttling through the condensing part of the turbine low-pressure end. In a new mill, a smaller DH turbine sizing, accounting for the partial DH generation in the flue gas condensers, will have higher pressure ratio at the same flow. This enables the steam to do more work in the turbine, for an outcome of clearly increased power generation.

In contrast to the Case C, in Case DH, the CAH and 2-stage scrubbing in Case S2 provides a clear increase in power generation for both retrofit and new mill cases. The CAH spray towers in these cases are sized for greater evaporation at approximately 60% of scrubbing water flow, 5°C temperature difference, and 25–30 kg/s evaporation rate. The lower the ΔT and the greater the evaporation, the greater the increase in power generation would be, but the size and cost would increase; we estimated that at the chosen level, the implementation could still be technically and economically feasible.

Finally, the heat pumps also proved useful for both retrofit and new mill cases, with over 4% and 6% power generation gains over the base case DH-D, respectively. The usefulness is also indicated by the relatively low COP and high ΔT_{lift} parameters that were found to yield the best results. Due to the different turbine back-end with a much greater combined swallowing capacity, no steam dumping was needed, even in the retrofit case.

CONCLUSIONS

The goal of this paper was to evaluate the potential to improve the power generation and energy efficiency of a kraft recovery boiler and the related steam cycle by improving the back-end heat recovery. We evaluated different configurations of spray tower-based condensing heat recovery schemes using IPSEpro process simulation software, and the evaluated cases included combustion air humidification (CAH) and heat pumps.

Lowering the recovery boiler flue gas temperature to 55°C–65°C decreases flue gas losses considerably. Significant amounts of energy could be recovered as hot water, which could then be used to reduce LP steam consumption. We found mixed results in terms of whether the heat recovered could be converted to net power generation gain, however. A key prerequisite is available swallowing capacity in the turbine for the saved LP steam made available. With the parameters we used in this study, even the simplest condensing heat recovery scheme was able to make more steam available for the condensing tail than it could accept.

The other conclusion is that combustion air humidification, used in many biomass boilers equipped with flue gas condensers, is not as clearly beneficial in a kraft recovery boiler due to the way the air preheating is implemented using extraction steam. The humidified air stream requires more steam for heating to prevent excessive drop of flue gas temperature, which in many cases partly or entirely negated any gain to be obtained from an increased amount and temperature level of heat recovery.

Despite the limitations, for a simple condensing plant, some 1%–4% additional electricity could still be generated. With a Nordic mill that provides district heating, a somewhat greater 4%–6% power generation gain could be achieved. In general, the profitability depends on finding suitable heat users where LP steam can be replaced by hot water, as well as having sufficient swallowing capacity available in the turbine to utilize the steam made available. While not considered in this study, it is also clear that if there is a market for increased heat sales, this can make condensing heat recovery schemes even more beneficial. For a new mill without bottlenecks in LP steam use, condensing heat recovery by implementing heat pumps appears promising. **TJ**

ACKNOWLEDGEMENTS

The authors gratefully acknowledge the funding from the Academy of Finland for the project “Role of forest industry transformation in energy efficiency improvement and reducing CO_2 emissions,” grant number 315019.

LITERATURE CITED

1. Vainio, E., Laurén, T., Demartini, N., et al., *J. Sci. Technol. For. Prod. Processes* 4(6): 14(2012).
2. Raukola, A., Ruohola, T., and Hakulinen, A., *Celulosa y Papel* 19(3): 6(2003).
3. Han, X., Yan, J., Karellas, S., et al., *Appl. Therm. Eng.* 110: 442(2017). https://doi.org/10.1016/j.applthermaleng.2016.08.178.
4. Liu, D., Jin, J., Gao, M., et al., *Int. J. Greenhouse Gas Control* 75: 74(2018). https://doi.org/10.1016/j.ijggc.2018.05.011.
5. Hebenstreit, B., Schnetzinger, R., Ohnmacht, R., et al., *Biomass Bioenergy* 71: 12(2014). https://doi.org/10.1016/j.biombioe.2014.01.048.
6. Terhan, M. and Comakli, K., *Appl. Therm. Eng.* 100: 1007(2016). https://doi.org/10.1016/j.applthermaleng.2015.12.122.
7. Teppler, M., Wood, J., and Buzzell, P., *PowerPlant Chem.* 11(2): 115(2009).
8. Blumberga, D., Vigants, E., and Veidenbergs, I., *Latv. J. Phys. Tech. Sci.* 48(4): 58(2011). https://doi.org/10.2478/v10047-011-0028-3.
9. Kuparinen K., Vakkilainen, E.K., and Hamaguchi, M., “Analysis on fossil fuel-free operation in a northern pulp and paper mill,” *Int. Chem. Recovery Conf.*, PAPTAC, Brossard, QC, Canada, 2017.
10. Vakkilainen, E.K., *Kraft Recovery Boilers: Principles and Practice*, Finnish Recovery Boiler Committee, Helsinki, 2005.
11. Tikka, P., *Chemical Pulping Part 2: Recovery of Chemicals and Energy*, Paper Engineers’ Association/Paper ja Puu, Helsinki, 2008.
12. Neto, M.R.V., Saari, J., Vakkilainen, E.K., et al., *J. Sci. Technol. For. Prod. Processes* 7(6): 36(2020).
13. Zaman, A. and Fricke, A., *Chem. Eng. Commun.* 155(1): 197(1996). https://doi.org/10.1080/00986449608936663.
14. Masse, M.A., Erdogan, K., and Fricke, A.L., *Polymer* 27(4): 619(1986). https://doi.org/10.1016/0032-3861(86)90249-1.
15. Saari, J., Kuparinen, K., Sermyagina, E., et al., *BioResources* 13(3): 5080(2018). https://doi.org/10.15376/biores.13.3.5080-5110.

16. Jüdes, M., Vigerske, S., and Tsatsaronis, G., “Optimization of the design and partial-load operation of power plants using mixed-integer nonlinear programming” in *Optimization in the Energy Industry*, Springer Berlin Heidelberg, Berlin, 2009, pp. 193-220. https://doi.org/10.1007/978-3-540-88965-6_9.

17. Sanders, W.P., *Turbine Steam Path Vol. 3a: Mechanical Design and Manufacture*, PennWell, Tulsa, OK, USA, 2004.

18. Traupel, W. *Thermische Turbomaschinen: 1. Thermodynamisch-Strömungstechnische Berechnung*, Springer-Verlag, Berlin, 1966. https://doi.org/10.1007/978-3-662-13209-8_1.

19. Veidenbergs, I., Blumberga, D., Vigants, E., et al., *Sci. J. Riga Tech. Univ.* 4(1): 109(2010). https://doi.org/10.2478/v10145-010-0025-4.

ABOUT THIS PAPER

Cite this article as:
Saari, J., Kaikko, J., Sermyagina, E., et al., *TAPPI J.* 22(3): 174(2023). https://doi.org/10.32964/TJ22.3.174

DOI: https://doi.org/10.32964/TJ22.3.174

ISSN: 0734-1415

Publisher: TAPPI Press

About this journal

ABOUT THE AUTHORS

We found the lack of studies and implementations of advanced condensing heat recovery solutions in recovery boilers a curious contrast to the fast-growing interest in such on other types of boilers. In this study, we considered several different cases, including retrofit and greenfield, as well as external heat sales.

The most difficult part of this study was that convergence performance of the simulation software was poor in several cases, making the calculation process often slow and tedious.

Through this study, we found that conclusions on condensing heat recovery in bubbling fluidized bed and circulating fluidized bed boilers do not translate to the recovery boiler context in a straightforward manner. Our most surprising finding was that the benefit of heat pumps and air humidification is not as clear in a recovery boiler as with other types of biomass boilers, but instead depends on a number of factors.

For mills, the study results indicate whether a mill considering an energy efficiency investment has a high chance of benefiting from condensing heat recovery in the recovery boiler. Based on the performance data, the next step would be to conduct a techno-economic study and optimization to obtain data on profitability and optimal configurations of heat recovery equipment.

Saari

Kaikko

Sermyagina

Hamaguchi

Cardoso

Vakkilainen

Haider

Saari is post-doctoral researcher, Kaikko is research director, Sermyagina is post-doctoral researcher, and Vakkilainen is professor in the Laboratory of Sustainable Energy Systems at Lappeenranta-Lahti University of Technology (LUT) in Lappeenranta, Finland. Hamaguchi is senior specialist at Stora Enso International Oy in Imatra, Finland. Cardoso is professor at the Federal University of Minas Gerais in Belo Horizonte, MG, Brazil. Haider is professor at Vienna University of Technology in Vienna, Austria. Email Saari at saari@lut.fi.